ChemComm

Accepted Manuscript

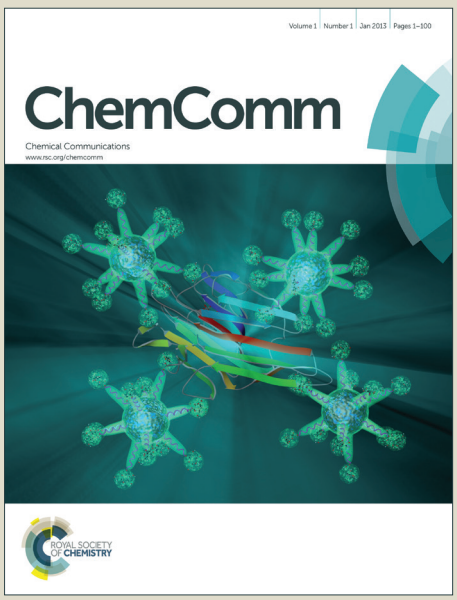

ROYAL SOCIETY OF CHEMISTRY

www.rsc.org/chemcomm

Chemical Communications

RSCPublishing

COMMUNICATION

Micropatterning of hydrophilic polyacrylamide brushes to resist cells adhesion but promote proteins retention

Cite this: DOI: 10.1039/x0xx00000x

Received 00th January 2012,
Accepted 00th January 2012

DOI: 10.1039/x0xx00000x

www.rsc.org/

Jianwen Hou,[ab] Qiang Shi,[a] Wei Ye,[ab] Paola Stagnaro[c] and Jinghua Yin[a]

Contrary to prevailing concept on protein adsorption and cell adhesion, a novel micropatterned polyacrylamide (PAAm) brushes that can resist cells adhesion but promote proteins retention is created through patterning of ATRP initiator and surface-initiated ATRP on polymer substrate.

Protein adsorption and cell adhesion are at the heart of many research fields.[1] Many approaches to regulate protein-material and cell-matrix interactions have been developed.[2] Among them, micropatterned polymer brushes with a controllable physic-chemical property at a molecular level have attracted much attention.[3] However, because the current strategy for controlling cell adhesion on patterned brushes is strictly based on the fouling properties of proteins,[4] polymer brushes cannot manipulate protein adsorption and cell adhesion in an opposite manner. The mixed adhesion of proteins and cells often disturbs proteomics and cell research, perplexes pharmaceutical screening processes and panel immunoassays, leading to misunderstandings the interaction of cells with substrates.[5] Thus, the selective adhesion of proteins and cells on polymer brushes is highly desirable.

The responses of proteins and cells to the surface are controlled by surface chemistry and topologies, as well as structure of polymer brushes.[6] Noncharged, hydrophilic and highly hydrated surfaces are good candidates for resistance of protein and cell.[6a] In contrast, conventional hydrogel can adsorb some proteins on its surface and entrap some proteins within its network.[5b] Inspired by these achievements, herein we find hydrophilic polymer brushes that possess hydrogel behaviors are good platforms with the capability to resist cell adhesion but promote protein retention. From the point of view of effectiveness, PAAm brushes should be the best choice. On the one hand, PAAm brushes highly resist protein and cell adhesion;[7] on the other hand, PAAm hydrogel shows the capability to mediate the protein entrapment.[8] In addition, densely-packed PAAm brushes grafted from the surface tend to gelatinize, because abundant hydrogen bonds of PAAm chains provide physical crosslinking in high density.[9]

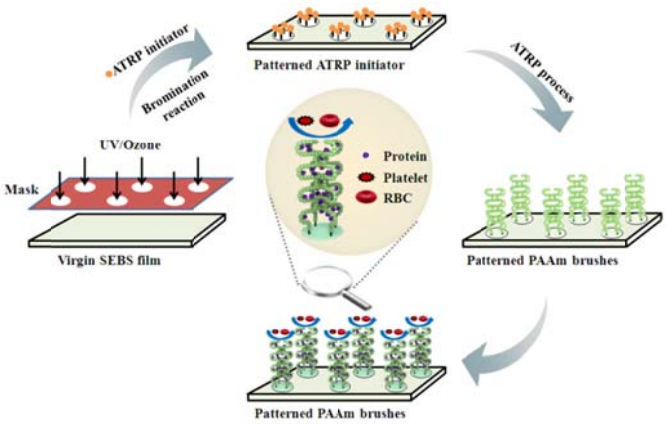

Scheme 1 Schematic diagram of creating patterned ATRP initiator on SEBS surface and subsequent SI-ATRP process to form patterned PAAm brushes over large areas. The patterned brushes exhibit extraordinary capability to promote protein retention and excellent resistance to blood cells adhesion.

Here, we fabricate the micropatternned PAAm brushes on a polymer substrate, styrene-b-(ethylene-co-butylene)-b-styrene elastomer (SEBS), to precisely manipulate the adhesion of plasma proteins and blood cells on the brushes. Plasma proteins and blood cells are selected because they play key roles in transport of oxygen and nutrients, coagulation for hemostasis and immunoprotection. In addition, blood-based detection, diagnosis of diseases and target drug delivery become urgently needed in recent years.[10] The patterned brushes are constructed by selective creation of ATRP initiator with photolithography, followed by SI-ATRP (Scheme 1). We demonstrate that the patterned PAAm brushes exhibit extraordinary capability to promote plasma

protein retention but resist blood cell adhesion. As a result, the patterned surface can effectively separate plasma proteins and blood cells from the fresh blood for real-time diagnosis in a one-step operation.

The patterned ATRP initiators on SEBS surface are *in situ* created by UV/Ozone irradiation through a copper photomask, followed by bromination with HBr/H_2SO_4 (5/1, v/v) solution (Scheme 1). The hydroxyl and carboxylic acid groups are formed in UV/Ozone exposed areas,[11] and become C-Br species after bromination, facilitating ATRP from the surface of SEBS.[12] The formation of hydroxyl, carboxylic acid groups and C-Br species is confirmed by the FTIR spectra and high-resolution spectra of XPS (Fig. S1 and S2, ESI†). The patterned PAAm brushes are then created from brominated SEBS via SI-ATRP. The presence of PAAm brushes grown from the ATRP initiator is evidenced by FTIR spectra (Fig. S1a, ESI†), XPS spectra (Fig. S1b and Fig. S2, ESI†) and AFM images (Fig. S3, ESI†), as well as the change of elemental composition on the sample surfaces (data are listed in Table S1, ESI†). PAAm brushes are covalently anchored to the SEBS surface with high grafting densities and packing densities, resulting in considerable stretching of the grafted chains from the substrate surface, as can be seen in higher-magnification SEM image (Fig. S4b, ESI†). There are many physical crosslinking in polymer brushes because of abundant intermolecular hydrogen bonds,[9] which render the polymer networks behave like polymer hydrogels (Scheme 1). And the rough and porous structures render the surface quite hydrophilic (water contact angle~21°) compared with hydrophobic surface (water contact angle~106°) of virgin SEBS film (Fig. S5, ESI†).

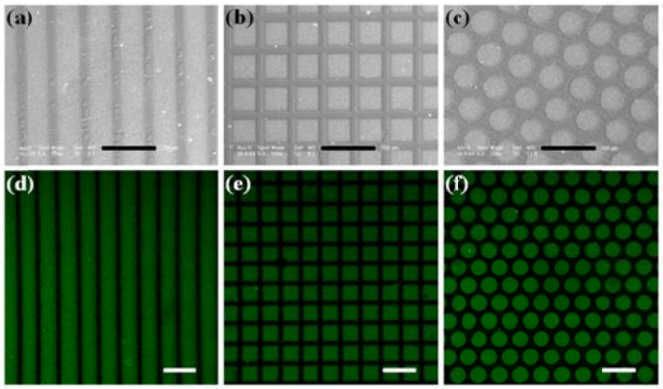

Fig. 1 SEM (a-c) and fluorescence (d-f) images of patterned PAAm brushes with varied geometries (stripe, square, and circle).

Fig. 1a-c show the SEM images of patterned surface with different shapes of PAAm brushes (stripe, square, and circle). The light areas are homogeneous PAAm brushes without visible defects. Inspection of higher magnification reveals dry polymer brushes are entangled to render the surface rough and porous, indicating polymer brushes behave like polymer hydrogels (Fig. S4b, ESI†). Interestingly, maybe due to the conjugated structure,[13] PAAm brushes prepared in this work exhibit fluorescence after excitation at 488 nm. As shown in Fig. 1d-f, the green fluorescent patterns of PAAm brushes are separated by dark backgrounds, in agreement with the patterns shown in POM images (Fig. S6, ESI†). These results demonstrate the patterned PAAm brushes have been successfully fabricated. In addition, the method presented here is versatile and reproducible, which creates multi-scale structure with various geometries over large areas.

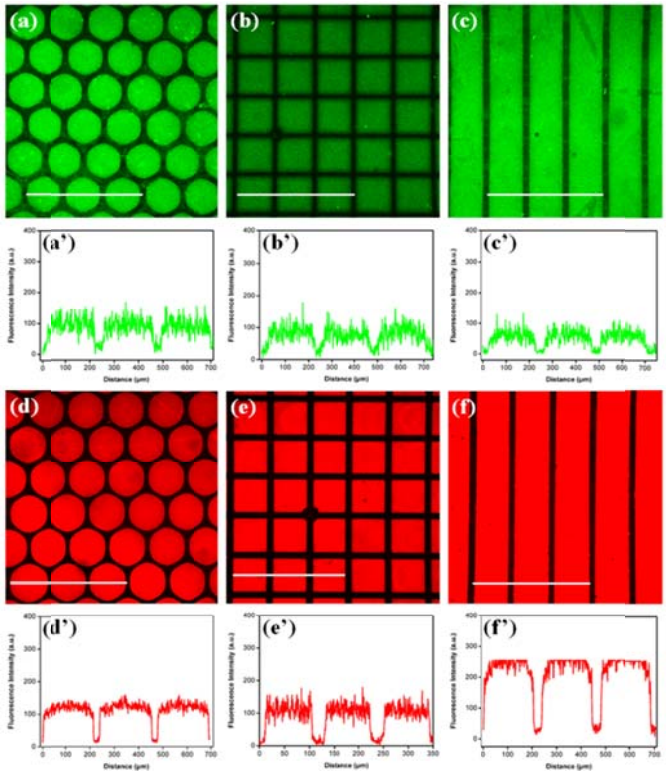

Fig. 2 Fluorescence micrographs of plasma protein patterns formed on the PAAm brushes. (a-c) FITC conjugated BFg, Lyz, and Hc. (d-f) RBITC conjugated BSA, BHb, and Tf. (a'-f') Line-profile graphs with peaks corresponding to the protein micropatterns indicated by the white line in a-f.

To check the capability of PAAm brushes to entrap proteins, six plasma proteins including bovine fibrinogen (BFg), lysozyme (Lyz), hemocyanin (Hc), bovine serum albumin (BSA), bovine hemoglobin (BHb) and transferrin (Tf), are selected as model proteins based on the size, molecular weight, charge of proteins and concentration in the plasma, which mainly determine their adsorption. The properties of model proteins are listed in Table S2 (ESI†). Fig. 2 shows fluorescence images of patterned surface after protein adsorption (a-f) and corresponding plots of fluorescence intensity (a'-f'). Compared with Fig. 1, the fluorescence intensity at microdomains of PAAm brushes increases substantially, indicating that plasma proteins are entrapped by PAAm brushes. To completely eliminate the influence of autofluorescence background of PAAm brushes, another three proteins are labeled with rhodamine B isothiocyannate (RBITC) (RBITC-BSA, RBITC-BHb and RBITC-Tf), because PAAm brushes do not show any

fluorescence in the detection wavelength range of RBITC, as can be seen in fluorescent micrographs (Fig. S7c, ESI†). Bright-red emission is clearly detected on PAAm microdomains (Fig. 2d-f) and the sizes of micropatterned polymer brushes have slight effects on the amount of protein retention, which can be seen in the fluorescent micrographs of FITC-BSA trapped by micropatterned polymer brushes with varied sizes (Fig. S8, ESI†). The above results confirm that PAAm brushes can entrap these plasma proteins and the encapsulating capacity is much stronger than the hydrophobic interaction between proteins and hydrophobic materials, which can be confirmed by the 3D CLSM images of the patterned brushes after protein entrapment (Fig. S9, ESI†). From fluorescence intensity, it is estimated that transferrin is entrapped by the polymer brushes with the highest density (Figure 3f').

The high capacity of PAAm brushes to capture proteins is believed to be the hydrogen bonds formation between PAAm brushes and proteins. It is well known that PAAm behaves as both hydrogen bond donors and acceptors.[14a] In addition, the peptide bonds of the protein can form multiple-point hydrogen bonds with AAm, which results in the strong interaction force between the protein and AAm.[14b] Furthermore, a hierarchical architecture is formed on the surface of SEBS driven by physical crosslinking in polymer brushes (Fig. S4b, ESI†). And this hierarchical architecture will offer more contact sites; in turn may contribute to the multiple-point hydrogen bond interaction between the proteins and PAAm brushes. Thus, a combination of hydrogen-bond interactions and surface topography is considered to jointly entrap the proteins in the PAAm brushes.[15] This unexpected capacity is of great significance because plasma proteins play key roles in multiple biological functions of human body. Therefore, patterned PAAm brushes can serve as ideal probes to monitor protein-protein interactions and protein-cell interactions.

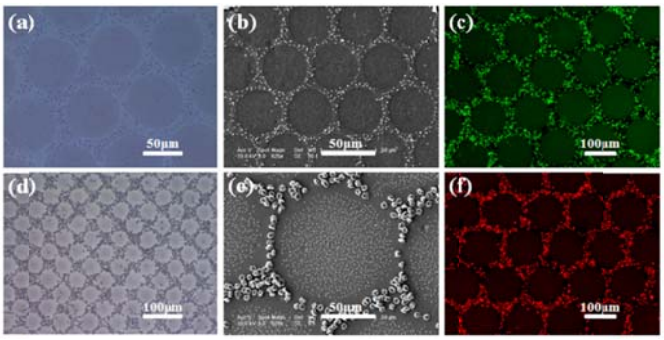

Fig. 3 POM (left), SEM (middle) and CLSM (right) images showing PLTs (a-c) and RBCs (d-f) adhesion on the micropatterned substrates, respectively.

To prove the resistance of polymer brushes toward blood cells, the adhesion of platelets (PLTs) and red blood cells (RBCs) on patterned surface is performed. Fig. 3a-c and 3d-f show the images (POM, SEM, CLSM) of the adhesion of platelets (PLTs) and red blood cells (RBCs) on the patterned surfaces, respectively. POM images show both cells tend to dominantly adhere to the annular regions outside PAAm brushes microdomains (Fig. 3a and 3d). SEM images show blood cells can be manipulated to single cells adhesion by simply decreasing the width of the annular hydrophobic regions (Fig. 3b, 3e and Fig. S10, ESI†). Interestingly, green fluorescent PLTs and red fluorescent RBCs can be observed by CLSM after excitation at 488 nm and 555 nm, respectively (Fig. 3c and 3f). CLSM images also support the resistance of PAAm brushes to the adhesion of blood cells. The pattern of blood cells on the surface is mainly caused by the hydrophobic interaction between the annular SEBS surfaces and the cells, while the highly hydrated PAAm chains in water can strongly repel cell adhesion on the substrate surface.[16]

The CLSM images show that the amount of proteins entrapped by PAAm brushes is much higher than that adsorbed on virgin SEBS regions. However, the result of cell adhesion is just the reverse. The number of blood cells (PLTs and RBCs) adhered on PAAm brushes is much lower than that on virgin SEBS regions. A further quantitative assessment of protein adsorption and cell adhesion on the surface of virgin SEBS and non-patterned PAAm grafted SEBS (SEBS-*g*-PAAm) is shown in Fig. S11 (ESI†). The amounts of proteins entrapped on the SEBS-*g*-PAAm surface are 1.5–3.5 times of that adsorbed on virgin SEBS surface. Compared with the virgin samples, SEBS-*g*-PAAm sample reduces about 91% and 96% of adhered RBCs and PLTs, respectively.

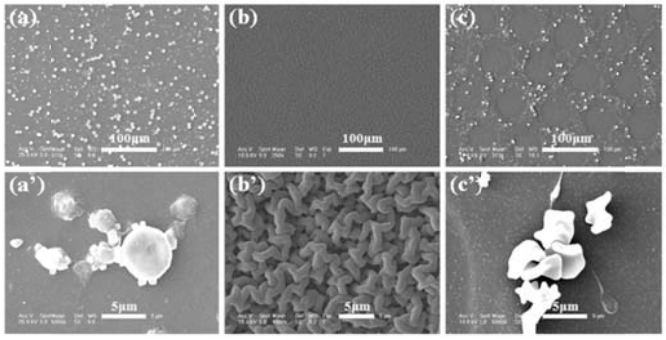

Fig. 4 Low and high magnification SEM images of blood cell adhesion from the whole blood on the surface of virgin SEBS (a, a'), SEBS-*g*-PAAm without patterning (b, b') and as-prepared patterned surface (c, c').

The adhesion of blood cells from fresh blood on three surfaces, virgin SEBS, non-patterned SEBS-*g*-PAAm and as-prepared patterned surface is completely different (Fig. 4). After incubation with blood at 37 °C for 1 h, RBCs and PLTs adhere randomly on the surface of virgin SEBS (Fig. 4a, 4a'). No blood cells are observed on the surface of SEBS-*g*-PAAm without pattern (Fig. 4b, 4b'). Exposure of the patterned SEBS-*g*-PAAm surface to whole blood results in the selective capture of PLTs and RBCs on the regions surrounding the PAAm patterns (Fig. 4c, 4c'). The patterned surface with PAAm brushes thus shows ability to separate proteins and cells in defined microenvironments, which could potentially be useful in

proteomic research, molecular recognition, bioelectronics, and clinical diagnostics.

In summary, by combining creation of patterned ATRP initiator and SI-ATRP, we have presented a facile protocol to micropattern PAAm brushes on the surface of SEBS with the capability of promoting protein retention but resisting to cell adhesion. Our strategy was based on patterned PAAm brushes behaving like the hydrogel can entrap protein while resist cell adhesion. The microstructure resulted in high fidelity patterns of plasma proteins and blood cells in separated areas on one SEBS surface. The patterned surfaces also precisely control the adhesion of blood cells down to the single-cell level. Our research paves new way on the design of biomedical devices and biomaterials to control protein and cell adhesion. These patterned polymer brushes provide multiple proteomic platforms that could be potentially applied in molecular recognition, biosensor and protein diagnostics.

This work was supported by the National Natural Science Foundation of China (51273199, 21274150 and 51103030).

Notes and references

[a] State Key Laboratory of Polymer Physics and Chemistry, Changchun Institute of Applied Chemistry, Chinese Academy of Sciences, Changchun, Jilin 130022, P. R. China
E-mail: shiqiang@ciac.ac.cn; yinjh@ciac.ac.cn
[b] University of the Chinese Academy of Sciences, Beijing 100039, P. R. China
[c]Istituto per lo Studio delle Macromolecole, UOS Genova, Via De Marini 6, 16149, Genova, Italy

Electronic Supplementary Information (ESI) available: [details of any supplementary information available should be included here]. See DOI: 10.1039/c000000x/

1 (*a*) G. A. Eggimann, E. Blattes, S. Buschor, R. Biswas, S. M. Kammer, T. Darbre and J. L. Reymond, *Chem. Commun.*, 2014, **50**, 7254; (*b*) H. K. Ravi, M. Stach, T. A. Soares, T. Darbre, J. L. Reymond and M. Cascella, *Chem. Commun.*, 2013, **49**, 8821; (*c*) K. Baumann, *Nat. Rev. Mol. Cell Biol.*, 2013, **14**, 404.
2 (*a*) H. Zhu, Z. Guo and W. Liu, *Chem. Commun.*, 2014, **50**, 3900; (*b*) P. Horcajada, T. Chalati, C. Serre, B. Gillet, C. Sebrie, T. Baati, J. F. Eubank, D. Heurtaux, P. Clayette and C. Kreuz, *Nat. Mater.*, 2010, **9**, 172; (*c*) M. A. Holden and P. S. Cremer, *J. Am. Chem. Soc.*, 2003, **125**, 8074.
3 (*a*) A. Olivier, F. Meyer, J.-M. Raquez, P. Damman and P. Dubois, *Prog. Polym. Sci.*, 2012, **37**, 157; (*b*) T. Chen, I. Amin and R. Jordan, *Chem. Soc. Rev.*, 2012, **41**, 3280; (*c*) D. J. Siegwart, J. K. Oh and K. Matyjaszewski, *Prog. Polym. Sci.*, 2012, **37**, 18; (*d*) T. Chen, R. Ferris, J. Zhang, R. Ducker and S. Zauscher, *Prog. Polym. Sci.*, 2010, **35**, 94; (*e*) M. CelesteáTria and J. YoungáPark, *Chem. Commun.*, 2011, **47**, 2393.
4 (*a*) R. Peng, X. Yao and J. Ding, *Biomaterials*, 2011, **32**, 8048; (*b*) M. S. Goel and S. L. Diamond, *Blood*, 2002, **100**, 3797; (*c*) S. F. van Dongen, P. Maiuri, E. Marie, C. Tribet and M. Piel, *Adv. Mater.*, 2013, **25**, 1687.
5 (*a*) J. B. Haun, N. K. Devaraj, S. A. Hilderbrand, H. Lee and R. Weissleder, *Nat. Nanotechnol.*, 2010, **5**, 660; (*b*) W. Yang, T. Bai, L. R. Carr, A. J. Keefe, J. Xu, H. Xue, C. A. Irvin, S. Chen, J. Wang and S. Jiang, *Biomaterials*, 2012, **33**, 7945.
6 (*a*) D. Rana and T. Matsuura, *Chem. Rev.*, 2010, **110**, 2448; (*b*) Q. Yu, L. M. Johnson and G. P. López, *Adv. Funct. Mater.*, 2014, **24**, 3751; (*c*) J. Zhao, L. Song, J. Yin and W. Ming, *Chem. Commun.*, 2013, **49**, 9191; (*d*) W. Ye, Q. Shi, S.-C. Wong, J. Hou, X. Xu and J. Yin, *Biomater. Sci.*, 2014, **2**, 1186.
7 F. Xu, K. Neoh and E. Kang, *Prog. Polym. Sci.*, 2009, **34**, 719.
8 P. Lu and Y.-L. Hsieh, *Polymer*, 2009, **50**, 3670.
9 (*a*) F. Ilmain, T. Tanaka and E. Kokufuta, *Nature*, 1991, **349**, 400; (*b*) W. Zhang, S. Zou, C. Wang and X. Zhang, *J. Phys. Chem. B*, 2000, **104**, 10258.
10 (*a*) X. Yu, Y. Zou, S. Horte, J. Janzen, J. N. Kizhakkedathu and D. E. Brooks, *Biomacromolecules*, 2013, **14**, 2611; (*b*) R. Yang, A. Garcia, D. Korystov, A. Mikhailovsky, G. C. Bazan and T.-Q. Nguyen, *J. Am. Chem. Soc.*, 2006, **128**, 16532. (*c*) Q. Shi, Q. Fan, W. Ye, J. Hou, S.-C. Wong, X. Xu and J. Yin, *ACS Appl. Mater. Interfaces*, 2014, **6**, 9808.
11 R. R. Bhat, B. N. Chaney, J. Rowley, A. Liebmann‐Vinson and J. Genzer, *Adv. Mater.*, 2005, **17**, 2802.
12 (*a*) J. F. Rabek and B. Rånby, *J. Polym. Sci., Part A: Polym. Chem.*, 1974, **12**, 273; (*b*) J. Hou, Q. Shi, P. Stagnaro, W. Ye, J. Jin, L. Conzatti and J. Yin, *Colloids Surf. B: Biointerfaces*, 2013, **111**, 333.
13 D. A. V. Bout, W.-T. Yip, D. Hu, D.-K. Fu, T. M. Swager and P. F. Barbara, *Science*, 1997, **277**, 1074.
14 (*a*) S. Y. Yang and M. F. Rubner, *J. Am. Chem. Soc.*, 2002, **124**, 2100. (*b*) X. Pang, G. Cheng, R. Li, S. Lu and Y. Zhang, *Anal. Chim. Acta*, 2005, **550**, 13.
15 (*a*) P. Roach, D. Farrar and C. C. Perry, *J. Am. Chem. Soc.*, 2006, **128**, 3939. (*b*) M. Ballauff, *Prog. Polym. Sci.*, 2007, **32**, 1135.
16 Q. Liu, A. Singh, R. Lalani and L. Liu, *Biomacromolecules*, 2012, **13**, 1086.

